N92-22364

SPACECRAFT-PLASMA INTERACTION CODES: NASCAP/GEO, NASCAP/LEO, POLAR, DynaPAC, and EPSAT

M. J. Mandell and G. A. Jongeward
Maxwell Laboratories/S-Cubed Division
P. O. Box 1620, La Jolla, CA 92038

D. L. Cooke
Phillips Laboratory/WSSI
Hanscom AFB, MA 01731-5000

Development of a computer code to simulate interactions between the surfaces of a geometrically complex spacecraft and the space plasma environment involves

(1) Defining the relevant physical phenomena and formulating them in appropriate levels of approximation;

(2) Defining a representation for the three-dimensional space external to the spacecraft and a means for defining the spacecraft surface geometry and embedding it in the surrounding space;

(3) Packaging the code so that it is easy and practical to use and to interpret and present the results;

(4) Validating the code by continual comparison with theoretical models, ground test data, and spaceflight experiments.

In this paper we discuss the physical content, geometrical capabilities, and application of five S-CUBED developed spacecraft plasma interaction codes. NASCAP/GEO is used to illustrate the role of electrostatic barrier formation in daylight spacecraft charging. NASCAP/LEO applications to the CHARGE-2 and SPEAR-1 rocket payloads are shown. DynaPAC application to the SPEAR-2 rocket payload is described. EPSAT is illustrated by application to TSS-1, SPEAR-3, and Sundance. The following paper contains a detailed description and application of the POLAR code.

1. INTRODUCTION

S-CUBED has been developing three-dimensional spacecraft-plasma interaction codes since the mid 1970's. During this time there have been great advances in computer hardware, in programming techniques, and in our understanding of the interactions between a spacecraft and its environment. (The latter has been aided by the availability of simulation codes.) Thus, succeeding codes have addressed ever more ambitious goals.

In this paper we briefly describe five S-CUBED developed spacecraft-plasma interaction codes. First, we discuss the physical phenomena we wish to model, their implications for spacecraft operations, and the consequent requirements on computer codes so that they may be used with relative ease and confidence for spacecraft design. Calculations illustrating the types of problems successfully solved will be presented for NASCAP/GEO, NASCAP/LEO, DynaPAC, and EPSAT. In the following paper (Cooke, 1991), David Cooke illustrates in more detail the use of the POLAR code.

2. PHYSICAL PHENOMENA

A uniform plasma satisfies the condition of vanishing space charge - otherwise its electrostatic potential would vary in accordance with Poisson's equation. At a boundary, however, the steady-state condition is to have vanishing net current. It follows that a spacecraft surface perturbs a plasma simply by its presence. Active spacecraft operations, such as applied surface potentials or effluents, serve to enhance that perturbation.

The plasma responds to the presence of a surface by providing currents to it. The incident plasma electrons and ions cause emission of low energy secondary electrons (Katz et al.,1986; Dekker, 1958; Hackenberg and Brauer, 1962; Gibbons, 1966; Dietz and Sheffield, 1975), which add to the photoemission (Feuerbacher and Fiton, 1972) caused by solar ultraviolet light. An insulating surface achieves steady state by reaching a potential at which the various current components are locally in balance. A conducting object (or set of objects) assumes a potential such that the currents balance when integrated over the surface.

The surface-plasma interaction described above is modified by many other effects. Spacecraft orbital motion leads to an inhomogeneous ram-wake structure in the space plasma. The geomagnetic field causes vxB potentials (Lilley et al., 1986) and magnetic insulation (Parker and Murphy, 1967). Plasmadynamic effects result from rapidly applied potentials, from beam operations, or simply from spacecraft caused plasma inhomogeneities. Effluents can be ionized, leading to plasma breakdowns and discharges.

3. CODE OBJECTIVES AND REQUIREMENTS

The objective of a spacecraft-plasma interaction code is to determine self-consistently the potentials and currents on the spacecraft surface and in the surrounding space. The results must be made available in a form which allows assessment of the consequences for spacecraft operations. Operations may be adversely affected by spacecraft charging in the geosynchronous and auroral environments. A high spacecraft floating potential may lead to unacceptable levels of parasitic currents, surface sputtering and contamination, or arcing. The optimal placement and acceptance angle of particle detectors is determined by the structure of the spacecraft sheath.

The first step in a simulation is to create or obtain a representation of the spacecraft surface. A calculation requires not only the geometrical configuration of the spacecraft surface, but also knowledge of the surface materials (in particular, their secondary emission properties) and how surface elements are

coupled electrically. A code must be able to model a large volume of surrounding space while maintaining adequate resolution for the phenomena of interest. It must also model a selection of boundary conditions to couple the spacecraft surface to its surrounding volume.

It is highly desirable that use of a computer code spread beyond its authors to the spacecraft science and engineering communities. This requires that thorough documentation be provided on the physical basis of the code as well as on its use. The initial step of creating a spacecraft surface representation must be reasonably convenient. Code input should be straightforward and user-friendly. Graphical and analytical post-processing tools must be available to aid in the interpretation and presentation of results.

To engender confidence in its calculations, the code should be able to reproduce theoretical and experimental results. For three-dimensional codes, the Child-Langmuir planar diode (Child, 1911) and the Langmuir-Blodgett spherical diode (Langmuir and Blodgett, 1924) are standard tests. Ground test experiments involving electron beams and plasma chambers test the code's ability to reproduce relatively well-controlled experimental results. Finally, spaceflight data from well-instrumented vehicles, notably the SCATHA satellite (Stevens and Pike, 1981), the DMSP series of spacecraft (Gussenhoven et al., 1985), and the SPEAR rocket experiments (Katz et al., 1989), validate the ability of the code to simulate plasma interactions under actual space conditions.

Each of the five S-CUBED developed computer codes discussed below was written with a specific primary purpose in mind, but can be used for a variety of aerospace and other applications. NASCAP/GEO (geosynchronous spacecraft charging) (Rubin et al., 1980), NASCAP/LEO (high voltage interactions with dense plasma) (Katz et al., 1981; Mandell et al., 1990a), POLAR (auroral spacecraft charging) (Cooke et al., 1985), and DynaPAC (dynamic plasma interactions) are fully three-dimensional and, among other things, solve some version of Poisson's equation in a large volume of space. EPSAT (Jongeward et al., 1990) differs in that it couples many environment and phenomenological models rather than solving differential equations.

4. NASCAP/GEO

NASCAP/GEO (NASA Charging Analyzer Program for Geosynchronous Earth Orbit) was developed for NASA/Lewis Research Center and the Air Force Geophysics Laboratory during the period 1976-1984. Its primary purpose was to model spacecraft charging in geosynchronous orbit. It has extensive particle tracking modules, including the ability to model electron beam irradiation, which was a popular way to simulate spacecraft charging in terrestrial laboratories.

The low level of plasma screening in the geosynchronous environment imposed the requirement of treating a large volume of empty space. NASCAP/GEO satisfies this requirement by a series of nested grids, each having half the physical dimension of its parent, with the spacecraft contained in the innermost grid. Finite element algorithms were developed to couple the grids with minimal loss of accuracy across the grid boundaries.

A very successful object definition module was written for NASCAP/GEO. Spacecraft were initially defined as collections of rectangular parallelepipeds, wedges, and tetrahedra, which fit comfortably in the cubic grid cells. A simple object definition language and graphical diagnostics made spacecraft surface definition very convenient, even with the crude computer hardware available at the time. Thin booms, thin plates, and transparent antennas were later added to the original cube-slice object repertoire. Figures 1 and 2 show examples of NASCAP/GEO spacecraft representations.

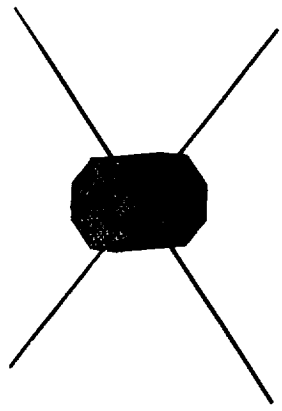

Figure 1. NASCAP/GEO representation of the SCATHA spacecraft.

NASCAP/GEO uses plasma and space charge representations appropriate to the geomagnetic substorm environment. NASCAP/GEO was used extensively to model earthbound electron beam irradiation experiments and flight measurements by the SCATHA spacecraft.

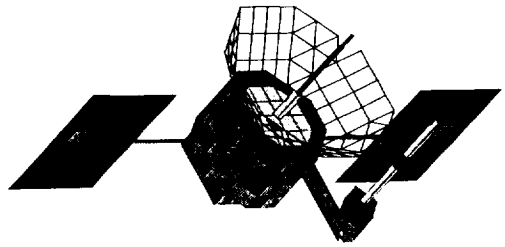

Figure 2. NASCAP/GEO representation of a communications satellite, showing thin plates, long booms, and a transparent antenna.

As an example of a NASCAP/GEO calculation, we present a simulation of a complex effect on a simple object: charging of an insulating sphere in sunlight due to formation of an electrostatic barrier (Mandell et al., 1978). Initially, the sunlit side of the sphere is "grounded" by photoelectron emission, while the dark side gradually charges negative due to incident plasma electrons. Eventually an electrostatic barrier forms to suppress the photoelectron emission, and the entire sphere charges to negative potential.

The NASCAP/GEO representation of a sphere as a twenty-six faceted object is shown in figure 3. Figure 4 shows the NASCAP/GEO produced potential structure around the sphere after the barrier has formed. The sun is incident from the upper right, and the potential field exhibits a saddle structure in front of the sunlit surface. Particle trajectories (figure 5), calculated using NASCAP/GEO's "DETECTOR" module, illustrate the effect of the barrier in blocking all but the highest energy photoelectrons.

Following barrier formation, the sunlit surface follows the dark surface in achieving high negative potential. As shown in figure 6, the process is characterized by a long time constant of

many minutes. This process has been observed on actual spacecraft (Olsen and Purvis, 1983).

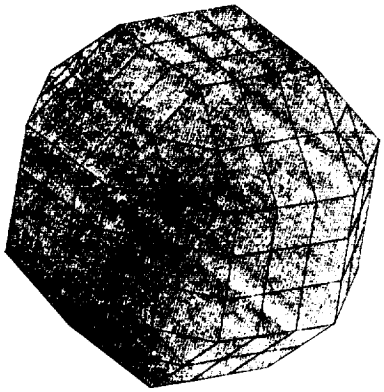

Figure 3. NASCAP/GEO representation of a sphere as a twenty-six faceted object.

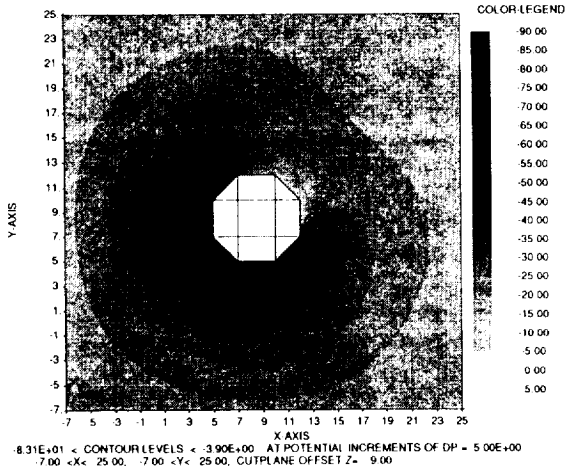

Figure 4. Potential structure around the sphere following barrier formation. Sunlight is incident from the upper right. The shaded surfaces are at -83 volts, the least negative surface potential is -4 volts, and the saddle point is at approximately -15 volts.

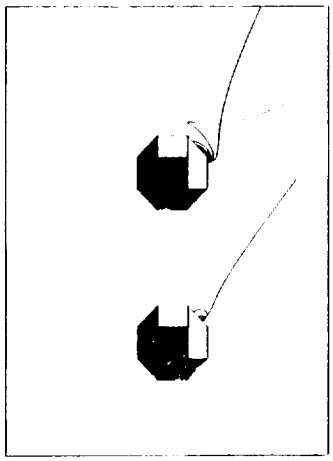

Figure 5. Particle trajectories for emitted photoelectrons of various energies. Only the most energetic electrons can escape over the electrostatic barrier.

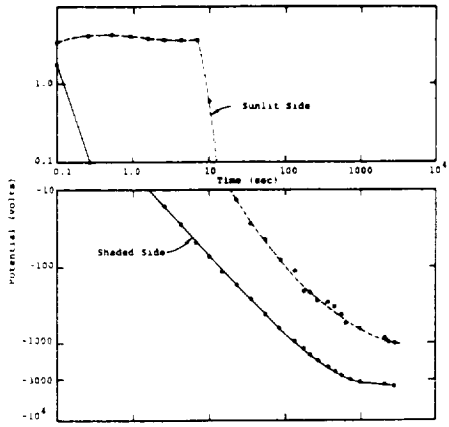

Figure 6. Time dependence of surface potentials for daylight charging.

5. NASCAP/LEO

NASCAP/LEO (Katz et al., 1981; Mandell et al., 1990a), was developed for NASA/Lewis Research Center during the period 1980-1990 for the purpose of studying plasma interactions in the dense, short Debye length plasma characterizing low- Earth orbit. It pioneered methods for embedding an arbitrary object (defined by industry-standard finite element pre-processors) in a cubic grid, with local subdivision for the resolution of small but important object features. It incorporates models for solar array surfaces, solar array circuitry, and hydrodynamic ion expansion. It has been applied to many plasma chamber experiments and rocket flights.

To avoid the need for obtaining space charge from particle simulations, NASCAP/LEO pioneered an analytic representation for space charge as a function of the local potential and electric field. The formula

$$\rho/\varepsilon_0 = -\left(\phi/\lambda_D{}^2\right)\left(1+|\phi/\theta|C(\phi,E)\right)/\left(1+(4\pi)^{1/2}|\phi/\theta|^{3/2}\right)$$

$$C(\phi,E) = |\theta/\phi|\left[\left(R_{sh}/r\right)^2 - 1\right]$$

$$\left(R_{sh}/r\right)^2 = 2.29\left|E\lambda_D/\theta\right|^{1.262}|\theta/\phi|^{.509}$$

reduces to linear screening for low potentials, and contains acceleration and convergence effects to reproduce a Langmuir-Blodgett spherical diode at high potentials.

NASCAP/LEO was used to perform a series of calculations for the CHARGE-2 rocket (Mandell et al., 1990b; Neubert et al., 1990). The CHARGE-2 mother vehicle could be held at a known negative potential by biasing it relative to the daughter, or taken to positive potential by electron beam emission. The electron and ion currents collected by the mother vehicle could be determined by measuring the tether current. The measurements compared well with NASCAP/LEO simulations.

In this paper we discuss performance of the "floating probes," which were intended to measure the vehicle potential and the sheath profile. Figure 7 shows the NASCAP/LEO model of CHARGE-2. (Note that, unlike a NASCAP/GEO object, the shape need not conform to the cubic grid.) The floating probes are seen extending up to one meter from the rocket surface. Under negative bias conditions, the potential of a floating probe is determined by equating the collected plasma ion current to the current through the 100 MΩ probe impedance.

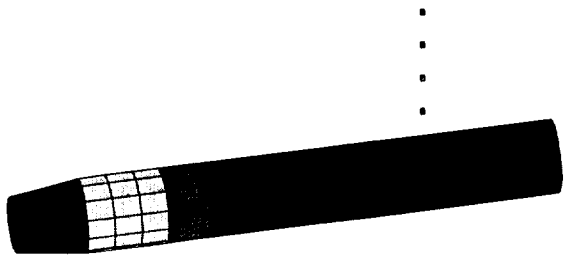

Figure 7. NASCAP/LEO model of CHARGE-2, showing floating probes.

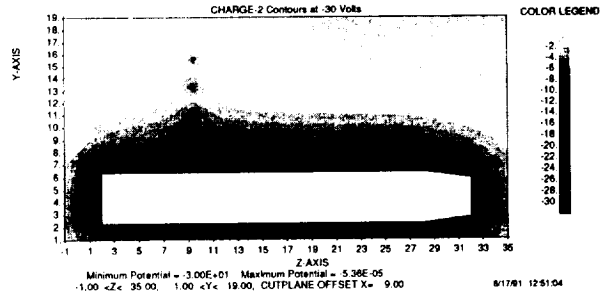

Figure 8. Potential around CHARGE-2 mother vehicle at -30 volts, showing perturbation by floating probes.

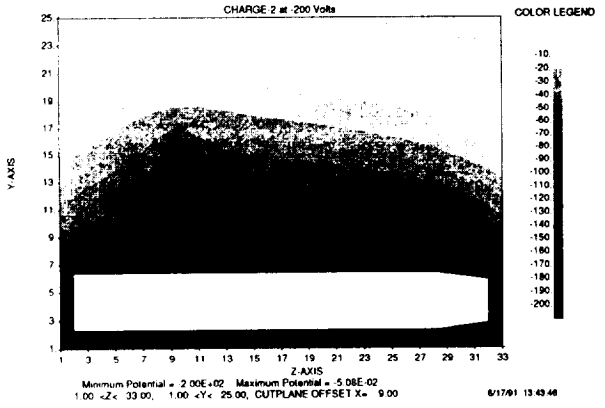

Figure 9. Potential around CHARGE-2 mother vehicle at -200 volts, showing floating probes inside the sheath.

Figure 8 shows the self-consistent potential structure with the mother vehicle at -30 volts. The probes are seen to produce a substantial sheath perturbation. Even though outside the sheath, the outermost probe cannot collect enough plasma ion current to provide an accurate potential measurement. Figure 9 shows the self-consistent potential structure with the mother vehicle at -200 volts. For this case, all of the probes are inside the sheath, and the 100 MΩ probe impedance essentially grounds the probes to the spacecraft. Figure 10 shows the calculated and experimental results for the spacecraft potential measured by the outermost probe as a function of the actual spacecraft potential (i.e., the tether bias). The floating probe measures about 70% of the actual potential up to about 20 volts. At higher spacecraft potentials, when the outermost probe is within the sheath, the measurement fails completely.

NASCAP/LEO played a crucial role in modeling the SPEAR-1 rocket experiment (Katz et al., 1989). SPEAR-1 (figure 11) contained two eight-inch diameter spheres which could be positively biased to a total of 45 kilovolts. A hollow cathode plasma contactor was intended to control the rocket body

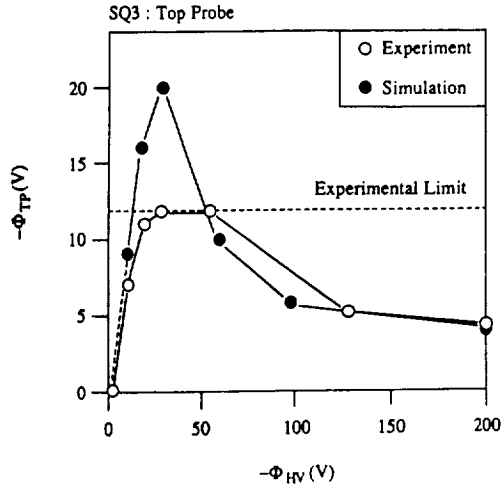

Figure 10. Experimental and NASCAP/LEO simulation results for the floating probe potential measurement vs. actual mother vehicle potential.

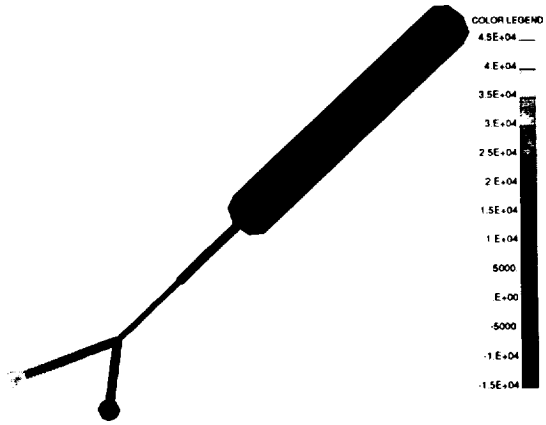

Figure 11. NASCAP/LEO model of the SPEAR-I rocket payload.

potential. With the failure of the hollow cathode door, this high voltage experiment became asymmetric and fully three-dimensional. The overlapping, bipolar sheath structure (figure 12) modified both ion collection by the rocket and magnetically limited electron collection by the sphere. NASCAP/LEO was used to calculate the electron and ion currents as a function of rocket potential, and thus determine the floating potential of the experiment.

Figure 13 shows a representative electron trajectory. If the sheath contours were concentric with the spherical probe, such an electron would ExB drift around a given potential contour and never be collected. In the actual case, however, the electron ExB drifts into a high field region and is collected by the sphere.

6. POLAR

The POLAR code (Cooke et al., 1985; Cooke, 1991) was developed for the Air Force Geophysics Laboratory during the time NASCAP/LEO was being written for NASA. POLAR was tuned for the auroral environment and for wake simulation. POLAR adopted an object definition language from NASCAP/GEO, and a dense plasma formulation from NASCAP/LEO. A "bread-slice" grid scheme was developed

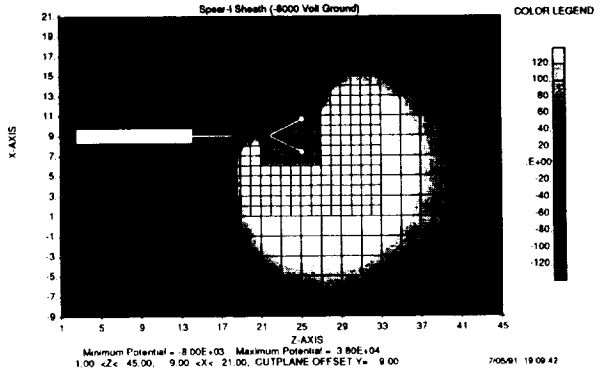

Figure 12. Bipolar sheath structure about SPEAR-I. (Sphere bias 45 kV, rocket potential -8 kV.)

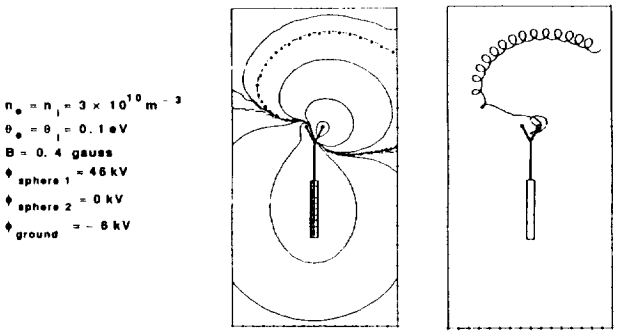

Figure 13. Potential contours and representative electron trajectory for SPEAR-1, showing failure of magnetic insulation due to sheath distortion.

so that the computational space could extend arbitrarily far into the wake of a spacecraft. The complex auroral charging environment is represented by a Fontheim fit (Fontheim et al., 1982). POLAR is able to correct the initially analytic space charge with particle trajectory data to achieve a self-consistent result, even in the presence of magnetic fields (Mandell et al., 1990b). In the following paper, David Cooke discusses more details about the POLAR code and its application to the DMSP satellites.

7. DynaPAC

DynaPAC, under development since 1989 for Geophysics Laboratory, Phillips Laboratory/WSSI, and SDIO, represents the next generation of three-dimensional code. It is being written for the computer hardware and the software techniques of the nineties. While it will be able to reproduce the results of the earlier codes, its primary focus is on dynamic effects for high power space applications. DynaPAC models space with arbitrarily nested cubic grids. Its high-order cubic elements provide more accurate potentials than the earlier codes and strictly continuous electric fields for particle tracking. Object definition, adapted from the NASCAP/LEO code, interfaces to industry-standard finite element preprocessors. Interactive screen interfaces make it easy to generate input for the DynaPAC modules. It is planned to include a selection of algorithms for various calculational tasks, so that a user can choose that most appropriate for his application, or use DynaPAC as a workbench for testing new algorithms. A programmer-friendly database language simplifies postprocessing tasks and construction of interfaces to other codes.

DynaPAC was used to model the SPEAR-2 payload tests in a very large vacuum chamber in PlumBrook, Ohio. SPEAR-2 contained a pulsed power system with voltages up to -100 kV and pulse widths up to 50 microseconds. By calculating the incident plasma currents to the high voltage components, DynaPAC predicted the observed anomalous measurement of the transformer secondary voltage in the presence of plasma.

The DynaPAC geometric model of SPEAR-2 (figure 14) clearly shows the high voltage components, including the pulse transformer, the klystrode battery pack, and, most prominently, the voltage divider probe used to measure the transformer secondary voltage. To calculate currents to the components, space is initially with a uniform ion distribution. DynaPAC then alternately solves for the space potentials and moves ions in those potentials, with the payload voltage following the prescribed risetime. By three microseconds (figure 15), ions are seen to be drained or expelled from high field regions, and to be converging on the voltage divider. The incident ion currents to the high voltage components (figure 16) are an order of magnitude higher than the equilibrium currents, which can be calculated either by NASCAP/LEO or by DynaPAC. Most of the incident ion current is to the high voltage end of the voltage divider probe. After adding the effects of ion- generated secondary electrons and evaluating the effect of the total injected current on the voltage divider circuit, we predicted that these currents would cause the transformer secondary voltage measurement to be low by about a factor of two. Experimentally, the measurement functioned nominally in vacuum, but was a factor of two low in plasma in agreement with the prediction.

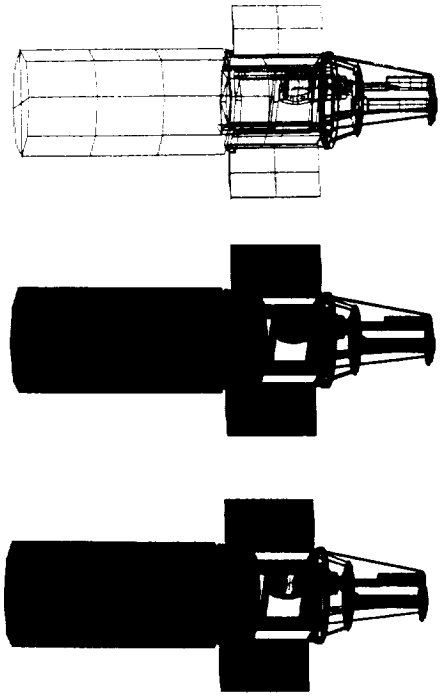

Figure 14. DynaPAC geometric model of SPEAR-2, showing wire-frame model (top), component-coded model (center), and potential-coded model (bottom).

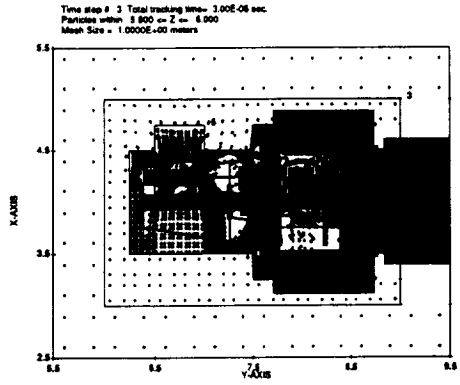

Figure 15. Ion macroparticle positions three microseconds into a SPEAR-2 high voltage pulse.

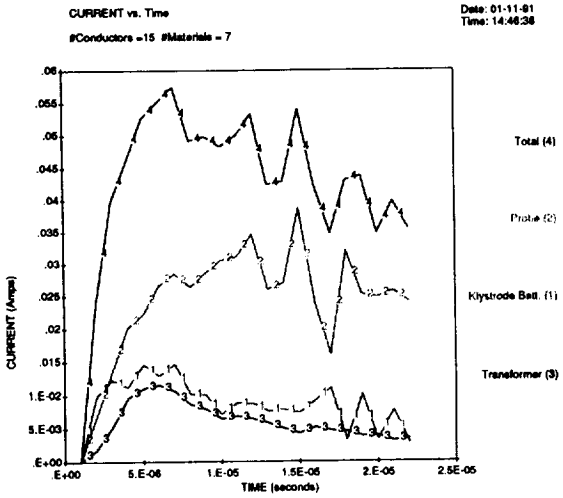

Figure 16. Time-dependent incident ion currents to the SPEAR-2 high voltage components.

8. EPSAT

EPSAT (Jongeward et al., 1990), under development since 1989 for NASA/Lewis Research Center and SDIO, is a very different type of code. Rather than solving three-dimensional equations, EPSAT uses simple, approximate analytic models to evaluate plasma interactions. An intelligent database couples a large number of interaction and environment models so that parameter studies are easily and efficiently performed.

EPSAT integrates quick running models into a unified desktop analysis tool (figure 17). The user has access to individual model results, such as the neutral environment at a point, or to coupled multi-step analyses, such as the total fluence of oxygen. EPSAT currently includes over one hundred models, many of which are shown in figure 18. The selection of models was based on the natural environment design needs for SDIO power systems. Desktop analysis tools for different applications can be constructed by appropriate addition or replacement of modules. A current project is development of an Environmental WorkBench for Space Station Freedom based on the EPSAT architecture.

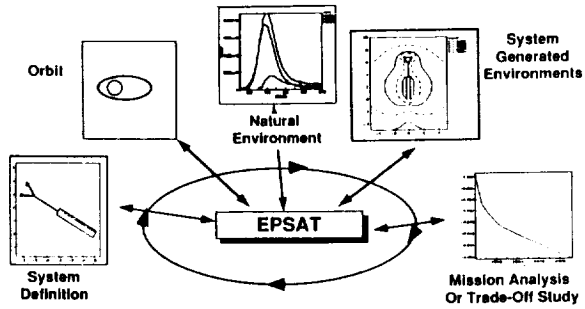

Figure 17. EPSAT integrates quick running models for orbits, environments, and interactions into a comprehensive desktop tool.

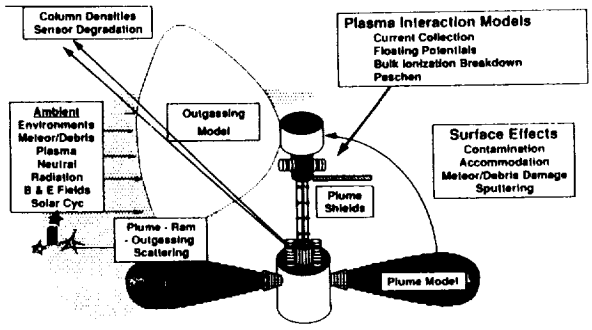

Figure 18. EPSAT has over one hundred models selected, based on natural environment design needs for SDIO power systems.

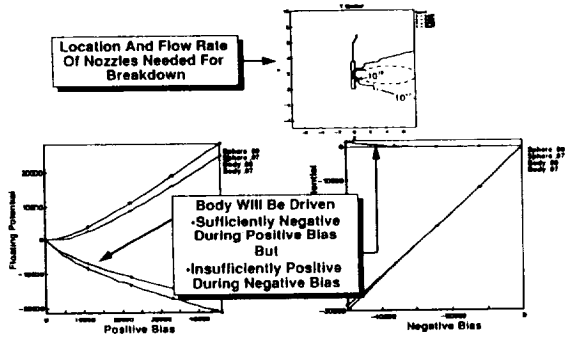

Figure 19. EPSAT was used to estimate floating potentials and effluent densities in the conceptual design of SPEAR-3.

EPSAT was used in the conceptual design of SPEAR-3. (See figure 19.) SPEAR-3 provides a test bed for spacecraft neutralization techniques. Rocket potential is provided by applying a high voltage to a SPEAR-1 type probe. EPSAT predicted that interesting negative potentials should be readily attained, but that only fairly small positive potentials could be achieved on the rocket. EPSAT was also used to predict effluent density profiles from gas release experiments.

At Phillips Laboratory (Boston) EPSAT was applied (M. Oberhardt, private communication) to the TSS-1 mission. (See figure 20.) High subsatellite potentials were predicted. Because only simplified analytic calculations are done, EPSAT can obtain results for many times during a mission, retrieving required parameters, such as plasma density or magnetic field, from accepted environment models. The floating potential plot reflects the night-day variation of plasma density and the diurnal magnetic field variation as the earth turns under the

orbit, and predicts a large variation in subsatellite potential. Also, the neutral density due to gas leaks appears to be high enough to lead to the possibility of breakdown.

Phillips Laboratory (Albuquerque) (B. Lillie, private communication) used EPSAT to examine the return flux of ACS effluent to optical sensors on the Sundance satellite. (See figure 21.)

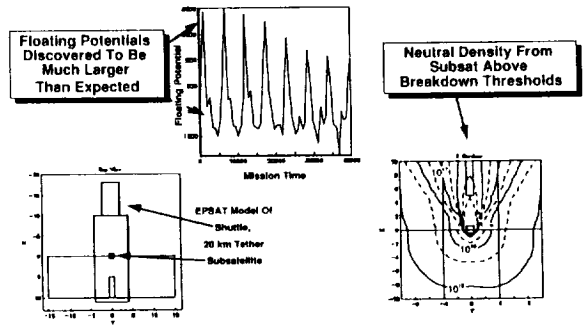

Figure 20. EPSAT was applied to the TSS-1 subsatellite to calculate orbital and diurnal potential variations and effluent densities.

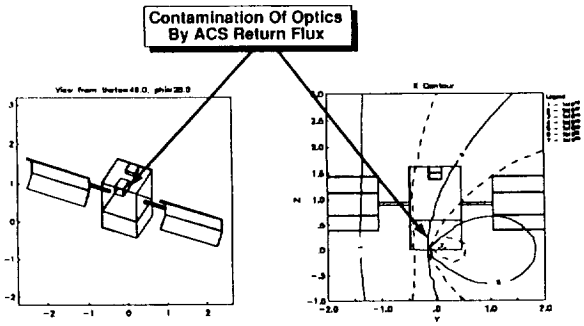

Figure 21. EPSAT was used to examine return flux of ACS effluent to optical sensors on the Sundance satellite.

9. CONCLUSION

It is practical and useful to simulate spacecraft-plasma interactions with three-dimensional, realistic geometry. The results are useful both for spacecraft design and for understanding and analysis of spaceflight data. Knowledge gained in the development and validation of three- dimensional codes has resulted in simplified interaction models which can be integrated with orbital and environment models in comprehensive design tools such as EPSAT. Appropriate simulations should be performed throughout the design phase of a spacecraft or space experiment to assure that no unexpected or harmful effects will occur due to interaction with the space environment.

REFERENCES

Child, C. D., "Discharge From Hot CaO," PHYSICAL REVIEW, 32, 492, 1911.

Cooke, D. L., "Validation and Applications of POLAR Code," 1991.

Cooke, D. L., Katz, I., Mandell, M. J., Lilley, Jr., J. R., and Rubin, A. J., "Three-Dimensional Calculation of Shuttle Charging in Polar Orbit," SPACECRAFT ENVIRONMENTAL INTERACTIONS TECHNOLOGY-1983, NASA CP2359, AFGL-TR-85-0018, 1985.

Dekker, A. J., "Secondary Electron Emission," SOLID STATE PHYSICS, 6, 1958, 251.

Dietz, L. A. and Sheffield, J. C., "Secondary Electron Emission Induced by 5-30-kev Monatomic Ions Striking Thin Oxide Films," JOURNAL OF APPLIED PHYSICS, 46, 4361-4370, 1975.

Feuerbacher, B., and Fiton, B., "Experimental Investigation of Photoemission from Satellite Surface Materials," JOURNAL OF APPLIED PHYSICS, 43, 1972, 1563.

Fontheim, E. G., Stasiewicz, K., Chandler, M. O., One, R. S. B., Gombosi, E., and Hoffman, R. A., "Statistical Study of Precipitating Electrons," JOURNAL OF GEOPHYSICAL RESEARCH, 87, A5, 1982.

Gibbons, D. J., "Secondary Electron Emission," HANDBOOK OF VACUUM PHYSICS, 2, 1966, 299.

Gussenhoven, M. S., Hardy, D. A., Rich, F., Burke, W. J., and Yeh, H.-C., "High-Level Spacecraft Charging in the Low-Altitude Polar Auroral Environment," JOURNAL OF GEOPHYSICAL RESEARCH, 90, 1985, 11009.

Hackenberg, O. and Brauer, W., Advances in Electronics and Electron Physics, 16, 1962, 145.

Jongeward, G. A., Kuharski, R. A., Kennedy, E. M., Wilcox, K. G., Stevens, N. J., Putnam, R. M., and Roche, J. C., "The Environment Power System Analysis Tool Development Program," CURRENT COLLECTION FROM SPACE PLASMAS, NASA CP3089, 1990.

Katz, I., Jongeward, G. A., Davis, V. A., Mandell, M. J., Kuharski, R. A., Lilley, Jr., J. R., Raitt, W. J., Cooke, D. L., Torbert, R. B., Larson, G., and Rau, D., "Structure of the Bipolar Plasma Sheath Generated By SPEAR I," JOURNAL OF GEOPHYSICAL RESEARCH, 94, 1989, 1450.

Katz, I., Mandell, M. J., Schnuelle, G. W., Parks, D. E., and Steen, P. G., "Plasma Collection by High-Voltage Spacecraft in Low Earth Orbit," JOURNAL OF SPACECRAFT AND ROCKETS, 18, 1981, 79.

Langmuir, I., and Blodgett, K. B. "Current Limited By Space Charge Flow Between Concentric Spheres," PHYSICS REVIEW, 24, 1924, 49.

Lilley, J. R. Jr., Katz, I., and Cooke, D. L., "V x B and Density Gradient Electric Fields Measured From Spacecraft," JOURNAL OF SPACECRAFT AND ROCKETS, 23, 1986, 656.

Mandell, M. J., Katz, I., Davis, V. A., and Kuharski, R. A., "NASCAP/LEO Calculations of Current Collection," CURRENT COLLECTION FROM SPACE PLASMAS, NASA CP3089, 1990a.

Mandell, M. J., Katz, I., Schnuelle, G. W., Steen, P. G., and Roche, J. C., "The Decrease in Effective Photocurrents due to Saddle Points in Electrostatic Potentials near Differentially Charged Spacecraft," IEEE TRANSACTIONS ON NUCLEAR SCIENCE, NS-25, 1978, 1313.

Mandell, M. J., Lilley, Jr., J. R., Katz, I., Neubert, T., and Myers, N. B., "Computer Modeling of Current Collection By the CHARGE-2 Mother Payload," GEOPHYSICAL RESEARCH LETTERS, 17, 1990b, 135.

Neubert, T., Mandell, M. J., Sasaki, S., Gilchrist, B. E., Banks, P. M., Williamson, P. R., Raitt, W. J., Meyers, N. B., Oyama, K. I., and Katz, I., "The Sheath Structure Around a Negatively Charged Rocket Payload," JOURNAL OF GEOPHYSICAL RESEARCH 95, 1990, 6155.

Olsen, R. C., and Purvis, C. K., "Observations of Charging Dynamics," JOURNAL OF GEOPHYSICAL RESEARCH 88, 1983, 5657.

Parker, L. W., and Murphy, B. L., "Potential Buildup on An Electron-Emitting Ionospheric Satellite," JOURNAL OF GEOPHYSICAL RESEARCH, 72, 1967, 1631.

Rubin, A. G., Katz, I., Mandell, M. J., Schnuelle, G., Steen, P., Parks, D., Cassidy, J. J., and Roche, J. C., "A Three-Dimensional Spacecraft-Charging Computer Code," SPACE SYSTEMS AND THEIR INTERACTIONS WITH EARTH'S SPACE ENVIRONMENT, H. B. Garrett, and C. P. Pike, ed., Progress in Astronautics and Aeronautics, Vol. 71, AIAA, 1980.

Stevens, N. J. and Pike, C. P., SPACECRAFT CHARGING TECHNOLOGY, 1980, NASA CP2182, 1981.